

# Prediction of Dynamic and Transient Rheological Properties of Polystyrene and High-Density Polyethylene Melts from the Molecular Weight Distribution

B. H. BERSTED, *Research and Development Department, Amoco Chemicals Corporation, Amoco Research Center, Naperville, Illinois 60540*

## Synopsis

A model relating the steady-shear melt viscosity and elasticity to the molecular weight distribution in HDPE and polystyrene melts has been extended to predict the dynamic viscosity, modulus, and loss modulus. Limitations in the model as applied to the dynamic properties are discussed. The model is also applied to the transient response of stress growth during steady shearing. This application is considered useful because it may help describe nonsteady-state flow of polymer melts in short dies and cyclic operations as employed in commercial molding equipment.

## INTRODUCTION

The dynamic properties of melts are useful in the characterization of polymer systems. The small-amplitude dynamic properties describe the elastic and viscous properties of a polymer melt and give a data base from which the relaxation spectrum can be calculated. From the relaxation spectrum, in turn, all linear viscoelastic behavior can be calculated. It is widely believed that the molecular weight and its distribution determine the terminal part of the relaxation spectrum and the small-amplitude dynamic properties; but up to now the detailed connection has not been made.

Transient experiments, such as the stress overshoot phenomenon in which the stress growth is measured at constant shear rate, are useful because they correspond more closely to conditions encountered in commercial processes than do the usual steady-state shearing experiments. For example, many commercial extrusion processes in injection and blow molding are operated with very short dies in which the steady-state shearing condition is not applicable, or the processes may be cyclic and of short duration.

The description of non-Newtonian flow properties has taken forms ranging from rather specific<sup>1-3</sup> molecular models to continuum models<sup>4-6</sup> capable of providing information on a wide variety of flows. In general, the continuum approaches have drawbacks because certain material-dependent parameters must be determined experimentally for each new sample. Network theories, such as that of Lodge,<sup>7</sup> also do not provide specific molecular information. Molecular models serve a supplementary role by accounting for the change in the material functions with molecular structure. Of the molecular models describing the response of polymer melts in simple shearing flow, Graessley's<sup>1</sup> has been the most successful. However, because his formulation is in terms of im-

plicit functions, the effect of molecular weight distribution, MWD, on viscoelastic response is not a direct one.

Recently, I proposed a model relating the viscoelastic response of polyethylene and polystyrene melts to the MWD.<sup>8,9</sup> The model assumes that the relaxation spectrum is progressively truncated with an increase in shear rate under steady shearing flow conditions. The maximum allowed relaxation time  $\tau_c$  (the relaxation time where the spectrum is truncated) is assumed to be only a function of shear rate:  $\tau_c = K/\dot{\gamma}$ , where  $K \simeq 2$ . The truncation of the relaxation spectrum, for a given molecular weight species  $M$  at any given shear rate results in the relaxation spectrum being essentially equivalent to that of a lower molecular weight homolog  $M_c(\dot{\gamma})$  at zero shear (its relaxation spectrum not being truncated), since the primary effect of molecular weight on the relaxation spectrum is only to extend the terminal relaxation portion. In other words, at this given shear rate the molecular species of molecular weight  $M$  acts as though it were of molecular weight  $M_c$ . The model was termed the "partition" model since all molecular species are partitioned by  $M_c$ . Because the shear-rate dependence of the relaxation spectrum was assumed to be only the effect of truncation, zero-shear (linear-viscoelastic) relationships for the melt viscosity, steady-shear elastic compliance, and first normal stress difference were used to calculate<sup>8,9</sup> these properties as a function of shear rate by including the shear-rate truncation of the relaxation spectrum.

Because my model successfully predicts the viscous and elastic responses of both polystyrene<sup>10</sup> and polyethylene melts undergoing steady shearing flow, I have now extended its application to see how well it describes oscillating and transient phenomena. The comparison of predicted and experimental small-amplitude oscillatory data tests the ability of the model to predict the relaxation spectrum from the MWD. I have also examined limitations to the predictions of this model from MWD data. Stress overshoot, though not an automatic consequence of the model, has been interpreted in terms of the model.

## EXPERIMENTAL

The samples were anionically polymerized polystyrene standards obtained from ArRo Laboratories; two high-density polyethylene (HDPE) samples previously<sup>9</sup> reported on; and Tenite 3340, the HDPE used by Chen and Bogue.<sup>11</sup>

The gel-permeation chromatography data were obtained at 135°C with trichlorobenzene as solvent on a Waters model 200 instrument having four styrogel columns with the following porosities:  $10^6$ ,  $10^5$ ,  $10^4$ , and  $10^3$  Å. The instrument calibration has been described.<sup>8</sup> Spreading corrections were applied<sup>10</sup> to the MWD of the polystyrene samples. MWD data are given in Table I.

TABLE I  
MWD of Samples Used in This Study

Sample	$\bar{M}_n, \times 10^{-3}$	$\bar{M}_w, \times 10^{-3}$	$\bar{M}_z, \times 10^{-3}$	$\bar{M}_w/\bar{M}_n$
PS-1	158	179		1.13
PS-2	86	96		1.11
HDPE Sample A	12.1	158	732	13.1
HDPE Sample B	28.2	148	559	5.2

## RESULTS AND DISCUSSION

## Calculation of the Dynamic Viscosity Storage and Loss Moduli

Relationships have been formulated<sup>9,10</sup> to relate the relaxation spectrum to MWD as

$$H(\tau_c) = \frac{d\eta}{d\tau_c} = \frac{K}{3.33\alpha} \frac{(\overline{M}_w^*)^{2.36} \overline{A}_2}{(M_c)^{2.33}} \left\{ 3.36 \left( \frac{\overline{M}_z^*}{\overline{M}_w^*} \right)^{0.51} + 1.02 \left( \frac{\overline{M}_z^*}{\overline{M}_w^*} \right)^{-0.49} \left[ \frac{M_c - \overline{M}_z^*}{\overline{M}_w^*} \right] \right\} \quad (1)$$

where

$$\overline{M}_w^* = \sum_{i=1}^{C-1} \overline{h}_i M_i + M_c \sum_{i=C}^{\infty} \overline{h}_i$$

$$\overline{M}_z^* = \frac{\sum_{i=1}^{C-1} \overline{h}_i M_i^2 + M_c^2 \sum_{i=C}^{\infty} \overline{h}_i}{\overline{M}_w^*}$$

$$\overline{A}_2 = \sum_{i=C}^{\infty} \overline{h}_i$$

and  $\tau_c = 1.4 \times 10^{-19} M_c^{3.33}$  for HDPE at 190°C. Also,

$$H(\tau_c) = \frac{d\eta}{d\tau_c} = \frac{3.4K}{3.84\alpha} \frac{(\overline{M}_w^*)^{2.4} \overline{A}_2}{(M_c)^{2.84}} \quad (2)$$

where  $\tau_c = 1 \times 10^{-21} M_c^{3.84}$  at 190°C for polystyrene. If these relationships are correct, the linear-viscoelastic functions ( $\eta'$ ,  $G'$ , and  $G''$ ) for small-amplitude oscillating shear should be predictable<sup>12</sup> from the well-known linear-viscoelastic relationships between the relaxation spectrum and  $\eta'$ ,  $G'$ , and  $G''$ .

Figures 1 and 2 give Graessley's experimental dynamic data for two previously studied HDPE samples<sup>9</sup> and my model's prediction. The good agreement between the experimental and predicted steady-shear viscosity and first normal stress difference as a function of shear rate lends credence to the relationship in eq. (1) for  $H(\tau)$ , from which the dynamic data were calculated. As no further adjustable parameters were used to predict the dynamic data, it can be concluded that the steady-shear and dynamic data can be interconverted. This verifies the transformation between the steady-shear viscosity and dynamic viscosity reported as an approximation of Graessley's model by Cote and Shida,<sup>13</sup> in which the MWD was not explicitly used.

As a first-order approximation of Graessley's theory Cote and Shida give

$$H(\tau)|_{\tau=2/\dot{\gamma}} = d\eta/d(2/\dot{\gamma}) \quad (3)$$

The present semiempirically derived model yields the relation

$$H(\tau)|_{\tau=1.7/\dot{\gamma}} = d\eta/d(1.7/\dot{\gamma}) \quad (4)$$

Figures 3 and 4 compare the experimental data of Porter and Prest<sup>14</sup> at 192°C for  $G'$ ,  $G''$ , and  $N_1$ , with the predictions at 190°C from the MWD of the narrow-MWD polystyrene with  $\overline{M}_w = 97,000$ . The coefficient,  $\alpha$ , obtained from the average of values calculated from  $J_e^0$  summarized in Graessley's review<sup>15</sup> on

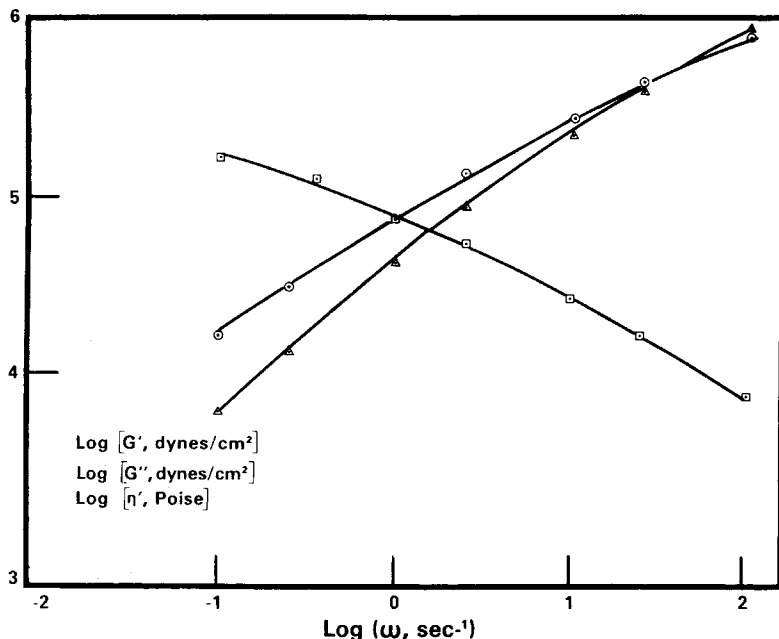


Fig. 1. The dynamic properties of HDPE sample A. The squares, circles, and triangles are experimental data of Graessley for  $\eta'(\omega)$ ,  $G''(\omega)$ , and  $G'(\omega)$  at 190°C. The solid lines are predicted from the model.

the entanglement concept, was determined to be  $1.5 \times 10^{-21}$  as compared to  $1 \times 10^{-21}$  reported previously,<sup>10</sup> based only on the data of Prest.<sup>16</sup> Agreement is very good at the lowest frequencies, but becomes progressively worse at higher frequencies. However, since the predictive model is based on idealized responses to steady shearing flow, which is dominated by the longest relaxation times, the poor agreement at high frequencies is understandable. These comparisons graphically illustrate that the "partition" model is limited to predicting properties based on terminal relaxations, and consequently is incapable of making predictions at high frequencies, where relaxation mechanisms associated with the chain lengths of the order of the entanglement length become important. The prediction for the HDPE samples given earlier was more successful because of polydispersity; the longer relaxation times tend to dominate the frequency range.

The polystyrene sample represented in Figures 3 and 4 was of relatively low molecular weight, and as such displayed an almost nonexistent plateau region. Figure 5 compares predicted and Graessley's experimental data at 141.6°C for a narrow-MWD polystyrene material of  $\bar{M}_w = 179,000$ . The constant  $K$  in the zero-shear viscosity relation was determined to be  $3.98 \times 10^{-11}$  from viscosity data on this material at 141.6°C. The proportionality constant  $\alpha$  between the relaxation time and the molecular weight to the 3.84 power, was calculated based on the temperature variation of the relaxation time  $\tau = \eta_0/\rho T$  using  $1.5 \times 10^{-21}$  for  $\alpha$  and  $1.585 \times 10^{-13}$  for  $K$  at 190°C. At 141.6°C,  $\alpha$  was calculated to be  $4.2 \times 10^{-19}$ . Figure 5 shows that the agreement is not as good as for the  $\bar{M}_w = 97,000$  material. However, the "partition" model predicts both an apparent shift of the terminal relaxations to longer times and an overall broadening, which arises

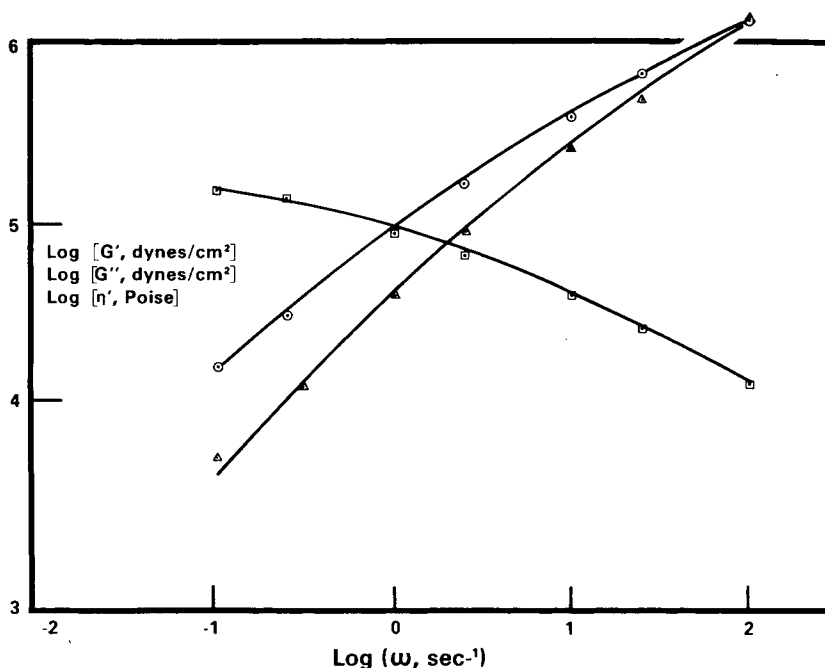


Fig. 2. The dynamic properties of HDPE sample B. The MWD and steady-shearing data for samples A and B have been reported elsewhere. The squares, circles, and triangles are experimental data of Graessley for  $\eta'(\omega)$ ,  $G'(\omega)$ , and  $G''(\omega)$  at 190°C. The solid lines are predicted from the model.

quite naturally out of the model's assumption that each molecule exhibits not only the longest relaxation mechanisms characteristic of its molecular weight, but also all relaxation mechanisms characteristic of lower molecular weight homologs.

The somewhat higher value for  $G'$  and  $G''$  in the plateau zone can readily be appreciated from a comparison reported earlier<sup>10</sup> between the relaxation spectrums calculated from the MWD and from the experimental dynamic data of Prest<sup>16</sup> for the  $\bar{M}_w = 411,000$  Pressure Chemical standard. The experimental data more closely approximate the "box" distribution. The predicted and experimental data agree at the terminal end, but the plateau region is not realized for the spectrum until smaller relaxation times for the predicted. Further, and perhaps more important, the ultimate plateau  $H(\tau)$  is larger for the predicted spectrum. I believe that this variance reveals a fundamental limitation of the "partition" model as formulated.

This problem is brought into sharper focus by considering the prediction of  $H(\tau)$  in terms of shear rate. Rearranging eq. (4) gives

$$H(\tau)|_{\tau=1.7/\dot{\gamma}} = \frac{-\dot{\gamma}^2 d\eta}{1.7 d\dot{\gamma}} \quad (5)$$

This relation, along with the predicted<sup>10</sup> power-law exponent of  $-0.885$  for polystyrene, shows that  $H(\tau)$  increases indefinitely with decreasing  $\tau$ , with no true plateau region. It is emphasized that polyethylene does not have this problem, as the predicted power-law exponent between  $\eta$  and  $\dot{\gamma}$  is ca.  $-1.0$ .

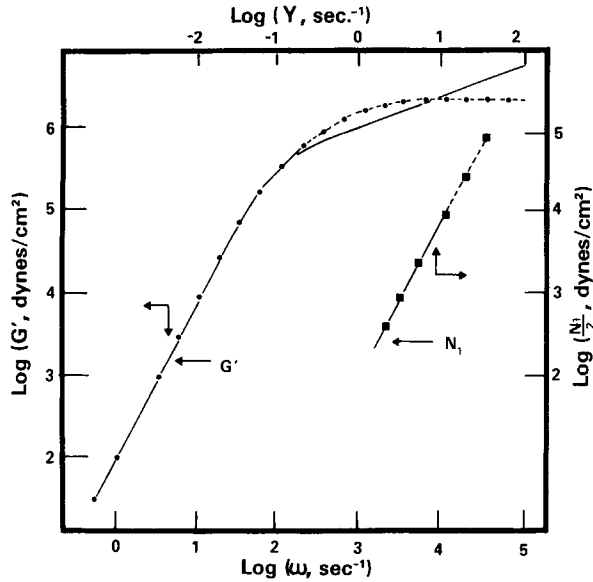


Fig. 3. The first normal stress difference  $N_1$  as a function of  $\dot{\gamma}$  and the dynamic storage modulus  $G'$  as a function of  $\omega$  for PS-2. The solid lines represent experimental data for the  $\bar{M}_w = 97,000$  Pressure Chemical polystyrene standard at  $192^\circ\text{C}$ . The closed squares and circles are points predicted from the model.

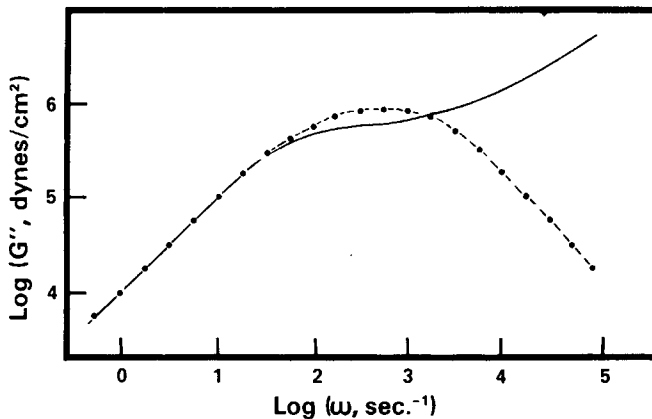


Fig. 4. The loss modulus  $G''$  as a function of  $\omega$ . The experimental data at  $192^\circ\text{C}$  of Prest and Porter (Ref. 14) for the  $\bar{M}_w = 97,000$  Pressure Chemical polystyrene standard (PS-2) are represented by the solid line and the solid circles with connecting dashed lines are the model's predictions.

However, because no narrow-MWD samples have been compared, it is difficult to judge this point. In order for eq. (5) to more faithfully mimic the relaxation spectrum, the limiting power-law exponent for polystyrene would have to be  $-1.0$ . In terms of the steady-shear viscosity for the narrow-MWD polystyrenes, the area of apparent conflict is the power-law region, where the power-law exponent of  $0.885$  does not seem unreasonably low. In fact, it is lower than has been estimated.<sup>17</sup> However, an even more fundamental reason for the variance may apply. Namely, that in making the calculation of eq. (5), I have assumed that the power-law region continues indefinitely as the shear rate increases and the

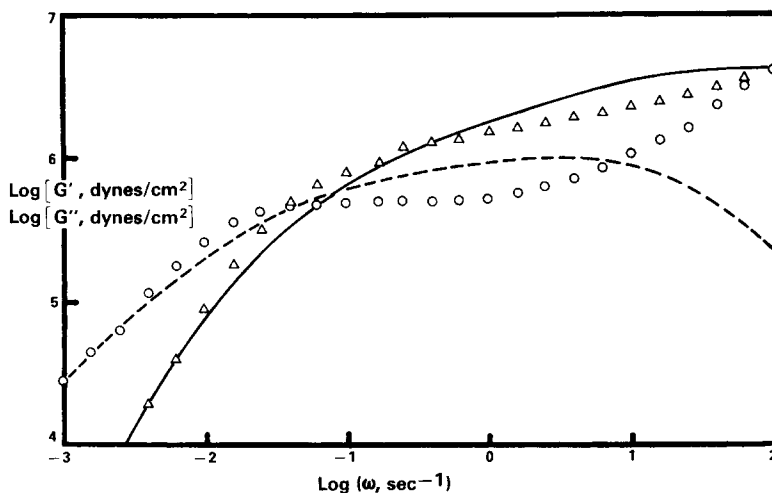


Fig. 5. The dynamic storage and loss moduli as a function of  $\omega$  for the Pressure Chemical polystyrene standard having  $\bar{M}_w = 179,000$  (PS-1). The solid and dashed lines are predicted from the present model, and the circles and triangles are experimental data from Graessley and Martin at 141.6°C for the dynamic loss and storage moduli, respectively.

largest allowed relaxation time decreases. Though the approximation may be valid for HDPE, where the entanglement molecular weight is quite low (ca. 4000), this is not a good approximation for polystyrene, where the entanglement molecular weight is approximately 30,000. The partition model obviously breaks down at this point.

While the reasons for the variance between the experimental and predicted dynamic data in the plateau region have been discussed, the modification of the "partition" model, in a manner consistent with the variety of data presented, is not obvious.

### Stress Overshoot

Stress overshoot at the onset of steady shearing flow has recently<sup>18,19</sup> been used to evaluate the different general continuum models. Evaluations of selected models are given in a review by Spriggs et al.<sup>20</sup> and by Chen and Bogue.<sup>11</sup> The Chen and Bogue approach gives reasonable agreement with experimental data. The more specific network-rupture model of Tanner<sup>21</sup> has also been shown to qualitatively account for the overshoot phenomenon.

The present model makes no obvious predictions regarding the stress-overshoot phenomenon. The maximum allowed relaxation time  $\tau_c$  at any shear rate  $\dot{\gamma}$  is assumed to be determined by the relation

$$\tau_c \cdot \dot{\gamma} = \text{const} \quad (6)$$

This relationship gives the largest active relaxation time for the steady-shear state, but not the rate of deactivation of the longest relaxation mechanisms in the approach to the steady state. To address this problem I will assume the time-dependent relaxation spectrum at the shear rate  $\dot{\gamma}$  as

$$H(\tau, \dot{\gamma}, t) = H(\tau, 0) \quad \text{for all } \tau \leq \tau_c \quad (7)$$

where  $H(\tau, 0)$  is the relaxation spectrum at zero shear rate and

$$H(\tau, \dot{\gamma}, t) = H(\tau, 0) \exp(-t/\tau_c) + H(\tau, \dot{\gamma}) [1 - \exp(-t/\tau_c)] \quad \text{for all } \tau > \tau_c \quad (8)$$

Equation 8 reduces to

$$H(\tau, \dot{\gamma}, t) = H(\tau, 0) \exp(-t/\tau_c) \quad \text{for all } \tau > \tau_c \quad (9)$$

since in the steady state for  $\tau > \tau_c$ ,  $H(\tau, \dot{\gamma}) \equiv 0$ . Equation 8 gives the time-dependent relaxation spectrum as a decay of the relaxation spectrum in the initial state  $H(\tau, 0)$  and a growth to the new state,  $H(\tau, \dot{\gamma})$ , with time constant  $\tau_c$ . Using the relations (7) and (9) together with the generalized linear model<sup>22</sup> for stress development at constant rate of strain, we get

$$\sigma(\dot{\gamma}, t) = \dot{\gamma} \int_0^{\tau_c} H(\tau, 0) [1 - \exp(-t/\tau)] d\tau \quad \text{for all } \tau \leq \tau_c \quad (10)$$

and

$$\sigma(\dot{\gamma}, t) = \dot{\gamma} \int_{\tau_c}^{\infty} H(\tau, 0) \exp(-t/\tau_c) [1 - \exp(-t/\tau)] d\tau \quad \text{for all } \tau > \tau_c \quad (11)$$

To compare predictions from this equation with the experimental data of Chen and Bogue,<sup>18</sup> certain parameters in eq. (1) must be evaluated at 160°C for  $H(\tau)$ . The constant in the zero-shear relation used at this temperature was calculated from that<sup>9</sup> at 190°C and an activation energy<sup>23</sup> of 6.3 kcal/mole. The zero-shear constant was calculated to be  $8.11 \times 10^{-13}$ . The relation between  $M_c$ , the largest molecular weight homolog still undergoing Newtonian flow at  $\dot{\gamma}$ , and shear rate was determined as described earlier<sup>8</sup> to be

$$M_c = 490,000 \dot{\gamma}^{-0.300} \quad (12)$$

The proportionality constant  $\alpha$  between the relaxation time and  $M^{3.33}$  was evaluated from the normal stress data of Chen and Bogue<sup>18</sup> as described elsewhere.<sup>9</sup>

Figure 6 compares the experimental data for stress development of Chen and Bogue<sup>11</sup> at 160°C and those predicted from the MWD using my model and the Bogue model.<sup>11</sup> The agreement for the position of the peak maximum at the two highest shear rates is moderately good. The quantitative comparison is not quite as good as that obtained from the Bogue model at the higher shear rates, but substantially better at the lowest shear rate. In fact, at the lowest shear rate my model does not predict an overshoot, in agreement with the experimental findings. The overshoot at the higher shear rates and the lack thereof at the lowest shear rate is a result of the competition as a function of time between the deactivation of relaxation mechanisms having  $\tau > \tau_c$  and the contributions of these relaxations to the stress as a function of time as predicted by linear-viscoelastic theory.

The first normal stress difference growth  $N(\dot{\gamma}, t)$  can also be calculated from the linear-viscoelastic relation<sup>24</sup> by the inclusion of a time-dependent relaxation spectrum as given in eqs. (7) and (9) as

$$N_1(\dot{\gamma}, t) = 2\dot{\gamma}^2 \int_0^{\tau_c} \tau H(\tau, 0) [1 - (1 + t/\tau) \exp(-t/\tau)] d\tau \quad \text{for all } \tau \leq \tau_c \quad (13)$$

and



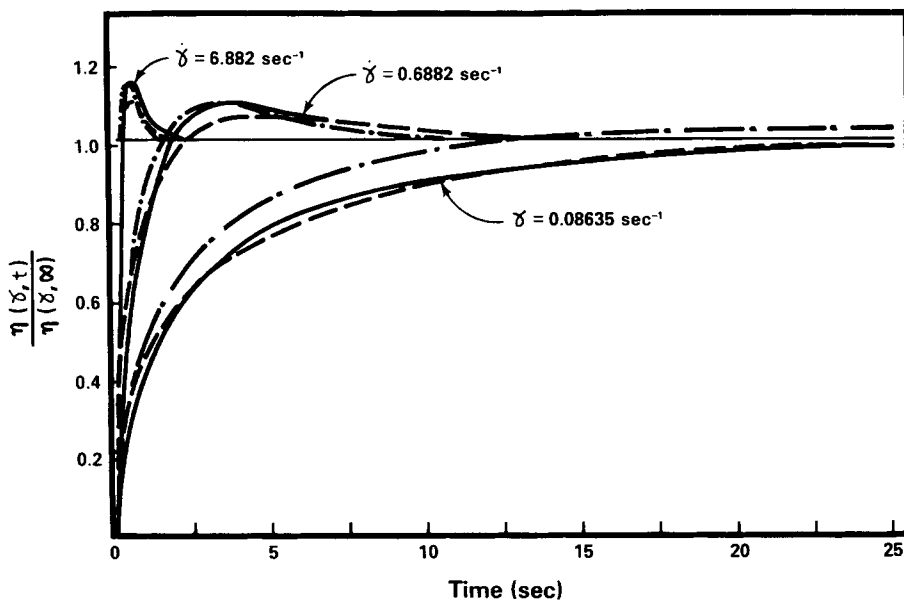


Fig. 6. Stress development at 160°C at the onset of steady shearing at constant shear rates. The solid curves represent the experimental data of Chen and Bogue (ref. 11), the dashed line is that predicted by the "partition" model, and the curve of alternating dashes and dots is that predicted by the Bogue (ref. 11) model.

$$N_1(\dot{\gamma}, t) = 2\dot{\gamma}^2 \int_{\tau_c}^{\infty} \tau H(\tau, 0) \exp(-t/\tau_c) [1 - (1 + t/\tau) \times \exp(-t/\tau)] d\tau \quad \text{for all } \tau > \tau_c \quad (14)$$

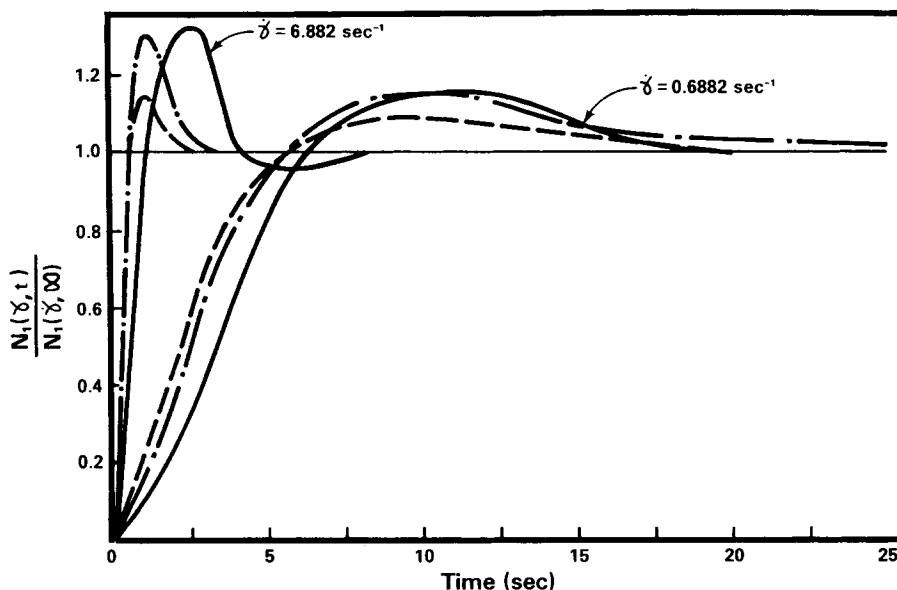


Fig. 7. First normal stress difference development curves at the onset of shearing at 160°C. The solid line is the experimental data of Chen and Bogue (ref. 18), the dashed line that predicted by the "partition" model, and the alternating dashes and dots the Bogue (ref. 18) model.

Figure 7 compares the experimental data of Chen and Bogue<sup>18</sup> with predictions of the Bogue model and those of eq. (14). Neither the Bogue model nor the predictions of eq. (14) quantitatively agree with the experimental data. However, certain features of the experimental data are reproduced using the above equation. First, the peak maximum for the normal stress difference is shifted to longer times relative to that in the shear-stress overshoot for both the predicted and experimental curves. Additionally, the overshoot peak is calculated to be broader for the normal stress overshoot than it is for the stress overshoot. This is qualitatively in agreement with the experimental data.

From the above comparisons, I conclude that the stress-overshoot phenomenon can be described reasonably well by the "partition" model. However, this description is not an automatic consequence of the model, because a new assumption about the time dependence of the relaxation spectrum must be made. It is interesting to note that both the predictions of my model and the experimental data on stress overshoot suggest that the time to reach the stress maximum  $t_m$ , is such that  $t_m \dot{\gamma} \simeq \text{const}$  total strain. This observation is accounted for quite naturally in the network-rupture model of Tanner.<sup>21</sup> For this reason, and because Tanner's model lends itself to the description, it seems a reasonable goal to combine the models so that the memory function of the "partition" model can be included in the network-rupture theory.

## CONCLUSIONS

The dynamic moduli for HDPEs having relatively broad MWDs are predictable from MWD data obtained by gel-permeation chromatography. Predictions of the dynamic moduli for narrow-MWD polystyrenes, however, demonstrate limitations of the "partition" model as presently formulated. Predictions in the terminal region agree quite well with experimental data, but agreement becomes worse in the plateau and transition regions. These limitations were not perceived in the steady-shear behavior of these materials, since the steady-shear responses depend heavily on the terminal relaxations.

The inability to correctly predict the dynamic moduli in the plateau and transition regions is not surprising, because relaxations depending on chain segments of the order of the entanglement length become important in these regions. My model is based on non-Newtonian behavior in steady shear and is therefore an entanglement model, which is oblivious to the relaxation times that depend on short segments having lengths less than interentanglement spacings.

Although the stress-overshoot phenomenon can be described moderately well by my model, the connection is not a direct one, and some serious differences between the predictions and the experimental data remain. Additionally, despite the somewhat arbitrary nature of the time-dependent relaxation spectrum, the concepts I have discussed may prove useful in the analysis of commercially interesting processes such as extrusion through dies of low  $L/D$ , where steady-state conditions do not prevail.

I would like to express my appreciation to Professor D. C. Bogue for the provision of the HDPE sample, for which published results on the overshoot phenomenon were available. I am also deeply indebted to Professor W. W. Graessley for supplying the dynamic rheological data on the polystyrene and polyethylene samples used, as well as for many useful discussions with him.

### References

1. W. W. Graessley, *J. Chem. Phys.*, **47**, 1942 (1967).
2. F. Bueche, *J. Chem. Phys.* **22**, 1570 (1954).
3. S. Middleman, *J. Appl. Polym. Sci.*, **11**, 417 (1967).
4. B. Bernstein, E. A. Kearsley, and L. Zapas, *Trans. Soc. Rheol.*, **9**, 27 (1965).
5. T. Spriggs, J. Huppler, and R. Bird, *Trans. Soc. Rheol.*, **10**, 191 (1966).
6. D. C. Bogue, *Ind. Eng. Chem. Fund.*, **5**, 253 (1966).
7. A. S. Lodge, *Trans. Faraday Soc.*, **52**, 120 (1956).
8. B. H. Bersted, *J. Appl. Polym. Sci.*, **19**, 2167 (1975).
9. B. H. Bersted, *J. Appl. Polym. Sci.*, **20**, 2705 (1976).
10. B. H. Bersted and J. D. Slee, *J. Appl. Polym. Sci.*, **21**, 2631 (1977).
11. I. Chen and D. C. Bogue, *Trans. Soc. Rheol.*, **16**, 59 (1972).
12. J. D. Ferry, *Viscoelastic Properties of Polymers*, Wiley, New York, 1970, p. 68.
13. J. Cote and M. Shida, *Trans. Soc. Rheol.*, **17**, 401 (1973).
14. W. Prest and R. Porter, *Polym. J.*, **4**, 154 (1973).
15. W. W. Graessley, *Adv. Polym. Sci.*, **16**, 65 (1974).
16. W. M. Prest, *Polym. J.*, **4**, 163 (1973).
17. R. Sabia, *J. Appl. Polym. Sci.*, **7**, 347, (1963).
18. I. Chen, Thesis, University of Tennessee, Univ. Microfilm No. 71-29, 453.
19. J. D. Huppler, T. F. MacDonald, E. Ashare, T. W. Spriggs, R. B. Bird, and L. A. Holmes, *Trans. Soc. Rheol.*, **11**, 181 (1967).
20. T. W. Spriggs, J. D. Huppler, and R. B. Bird, *Trans. Soc. Rheol.*, **10**, 191 (1966).
21. R. I. Tanner, *Chen. Eng. Sci.*, **22**, 1803 (1967).
22. J. D. Ferry, *Viscoelastic Properties of Polymers*, Wiley, New York, 1970, p. 77.
23. R. Porter, J. R. Knox, and J. Johnson, *Trans. Soc. Rheol.*, **12**, 409 (1968).
24. F. H. Gortemaker, M. Hansen, B. deCindio, H. Laun, and H. Janeschitz-Kriegl, *Rheol. Acta*, **15**, 267 (1967).

Received August 2, 1977

Revised February 3, 1978